Single-step laser-based fabrication and patterning of cell-encapsulated alginate microbeads

DM Kingsley[1], **AD Dias**[1], **DB Chrisey**[2], and **DT Corr**[1,*]

[1]Department of Biomedical Engineering, Rensselaer Polytechnic Institute, 110 Eighth St., Troy, NY 12180, USA

[2]Department of Physics, Tulane University, 6823 St. Charles Avenue New Orleans, LA 70118, USA

Abstract

Alginate can be used to encapsulate mammalian cells and for the slow release of small molecules. Packaging alginate as microbead structures allows customizable delivery for tissue engineering, drug release, or contrast agents for imaging. However, state-of-the-art microbead fabrication has limited range in achievable bead sizes, and poor control over bead placement, which may be desired to localize cellular signaling or delivery. Herein, we present a novel, laser-based method for single-step fabrication and precise planar placement of alginate microbeads. Our results show that bead size is controllable within 8%, and fabricated microbeads can remain immobilized within 2% of their target placement. Demonstration of this technique using human breast cancer cells shows that cells encapsulated within these microbeads survive at a rate of 89.6%, decreasing to 84.3% after five days in culture. Infusing rhodamine dye into microbeads prior to fluorescent microscopy shows their 3D spheroidal geometry and the ability to sequester small molecules. Microbead fabrication and patterning is compatible with conventional cellular transfer and patterning by laser direct-write, allowing location-based cellular studies. While this method can also be used to fabricate microbeads *en masse* for collection, the greatest value to tissue engineering and drug delivery studies and applications lies in the pattern registry of printed microbeads.

Keywords

Alginate; High-Throughput; Laser; Micropatterning; Microsphere; Microencapsulation

1. Introduction

Microbeads are three-dimensional, generally spherical microstructures that are currently being investigated for applications in tissue engineering and for delivery of drugs, contrast agents, proteins, and DNA [1,2]. The permeability [3], biocompatibility [4], mechanical properties [5], and degradation kinetics [6] of microbeads are important design parameters to optimize their utility. Microbead permeability has implications in diffusion kinetics, and it has even been tailored to give microbeads selective permeability for specific soluble factors [7]. The mechanical properties of microbeads influence mechanotransduction, so controlling parameters such as elastic modulus may impart signals to encapsulated cells [8]. The *in situ* degradation kinetics are critically important for sustained drug delivery and for tissue

*Corresponding author. David T Corr, Ph.D., Associate Professor, Department of Biomedical Engineering, Rensselaer Polytechnic Institute, 110 8th Street, Troy, NY 12180, Phone: (518) 276-3276, Fax: (518) 276-3035, corrd@rpi.edu.

engineering applications where the scaffold has a desired lifetime. To control these properties, hydrogels have become widely used in microbead applications because of their customizability. Typical hydrogel materials include collagen, hyaluronan, alginate, and synthetic polymers such as poly-ethylene glycol [9]. In particular, alginate has become a popular hydrogel for fabricating cell-encapsulating microbeads [8,10], because of its biocompatibility and mechanical properties that can be tuned within physiologic values.

Microbeads can be used to sequester soluble molecules [11] and encapsulate cells [12–14]. These capabilities are used in tissue engineering and regenerative medicine to selectively differentiate stem cells [15–17] and create soluble factor concentration gradients to guide cell migration [18,19]. One of the primary advantages of microbeads over bulk scaffolds for tissue engineering applications is that the surface area-to-volume ratio is small enough to allow rapid transport of nutrients and waste of the encapsulated cells [20].

Recent microbead fabrication devices take advantage of alginate's unique property of crosslinking in the presence of divalent cations such as calcium. Electrostatic bead generators have shown success in fabricating microbeads by using an electric field to extrude droplets of alginate into baths of calcium chloride solution. To increase the size of fabricated beads, higher electric field strengths are utilized, resulting in larger-diameter beads [1]. Other technologies have focused on using microfluidic devices [13,21,22] or micro-vibrators [23] to generate alginate droplets which crosslink when they contact calcium chloride solution. Microbead size can be adjusted by changing the flow rate [21,22,24] or air pulse frequency [13] inside the device. Additional methods for microbead fabrication include using high-pressure nozzles or syringe needles to expel alginate into calcium chloride solution [25,26].

Despite their ability to create beads of controlled size, microfluidic, electrostatic, and pressure-based bead generators cannot precisely control microbead placement. These techniques can fabricate monodispersed beads [1,12,21,22], yet the placement of beads at controlled distances has not been demonstrated. Accurate bead placement in micropatterns can enable custom tissue-engineered constructs of loaded microbeads or precise delivery of small molecules, as well as the spatial precision necessary to modulate paracrine cellular signaling. Lithography-based patterning techniques are precise, but involve high temperatures, high pressures, and various chemicals that would not be compatible with microbeads that encapsulate viable cells [27] or temperature-sensitive molecules like proteins or nucleic acids. One method for patterning microbeads with viable cells uses an optically switched dielectrophoretic (ODEP) force to manipulate alginate beads [28]. However, this technique, like many others, cannot be easily used to manipulate single beads. For especially precise applications in tissue engineering and regenerative medicine, it is often important to pattern single beads with viable cells.

Laser direct-write (LDW) has been used as a tool for creating patterns of single [29] or multiple [30] microbeads. To date, these techniques require pre-fabricated beads, are unable to pattern large beads (over 250 μm), and have limited pattern resolution. Moreover, when utilizing LDW to pattern prefabricated cell-loaded microbeads, cell viability inside of the microbeads dropped substantially during the printing process [29]. Another laser-based technique for microbead formation, laser-induced forward transfer (LIFT), does not offer the necessary control over bead size and placement [31]. An additional consequence of this technique is the generation of unwanted satellite microbeads, possibly due to a large alginate travel distance required for foil-based ejection and circular bead formation. Due to their precision and controllability, laser-based printing techniques have excellent resolution for cell printing [32,33], even using alginate for 3D microscaffolds [34]. LDW has not been previously shown to generate microbeads. In this paper, we present a novel microbead

fabrication technique that utilizes LDW as a single step to both fabricate and place single alginate microbeads in spatial patterns with micron-level precision.

2. Materials and Methods

2.1. Cell culture

GFP-labeled MDA-MB-231-gfp (M231) human breast cancer cells (ATCC, Manassas, VA) were grown in standard cell culture conditions (37 C, 5% CO_2, 95% RH) in growth medium consisting of Dulbecco's Modified Eagle's Medium (DMEM) supplemented with 10% (v/v) fetal bovine serum (FBS), 100 U/ml penicillin/streptomycin, and 2 mM L-glutamine. Human foreskin fibroblasts (HFF-1, ATCC) were transduced with mCherry crude lentiviral particle (GeneCopoeia, Rockville, MD) and cultured in DMEM supplemented with 10% (v/v) FBS and 100 U/ml penicillin/streptomycin.

2.2. Laser-based microbead fabrication

A LDW system [32] was adapted to fabricate alginate microbeads (Fig. 1). To prepare alginate for cross-linking into microbeads, alginic acid sodium salt (Sigma Aldrich, St. Louis, MO) was dissolved slowly into cell culture grade distilled water at 2% w/v along with sodium chloride at 0.9% w/v. The alginate solution was stirred overnight and passed through 0.8 μm and 0.2 μm cellulose acetate filters.

To prepare a receiving substrate for microbead cross-linking and immobilization, poly-L-lysine (MW 70000–150000; Sigma Aldrich, St. Louis, MO)-coated Petri dishes were spin coated with warm 10% gelatin/2% calcium chloride at 2000 rpm for 20 seconds. After a five minute refrigeration, the dish was rinsed with cold 2% calcium chloride and placed in a 37° C-incubator for 25 minutes. To prepare the print ribbon for material deposition, a flat, 50-mm diameter, UV-transparent quartz disk ("ribbon"; Edmund Optics, Barrington, NJ) was spin coated with 10% gelatin/2% alginate solution at 2000 rpm for 20 s. The ribbon was then incubated at 37° C for 3 minutes. To load the print ribbon, M231 cells, suspended in 2% alginate/0.9% sodium chloride, were pipetted onto the prepared ribbon and incubated for 7 minutes, then moved to a laminar flow hood for 4 minutes. Excess alginate was removed, and the ribbon was inverted and mounted approximately 750 μm above the receiving substrate in the LDW system (Teosys LLC, Crofton, MD) [32]. The receiving substrate and mounted ribbon were secured on independent x-y Computer-Aided Design/Computer-Aided Manufacturing (CAD/CAM)-controlled motorized stages. A program was used to pulse the laser (ArF excimer; λ=193 nm) once for each corresponding target spot and deposit M231 cells and 2% alginate solution onto the receiving dish, where the deposited droplets crosslinked *in situ*, forming microbeads. After each microbead was printed, the receiving stage and ribbon stage were each independently moved so the next alginate droplet could be placed on the receiving substrate according to the program. A charged coupled device (CCD) camera sharing the beam path with the laser [32] allowed real-time focusing and selection of desired cells to be encapsulated in the printed beads.

To rapidly perform bead fabrication, the receiving stage was moved at an average velocity of 600 μm/s to the next programmed location at a linear distance of 600 μm, with no pauses in movement. Cell-containing alginate microbeads on the receiving dish were incubated for 10 minutes after the transfer was completed. Media was then added for cell survival.

2.3. Control and characterization of microbeads and patterns

The size of the fabricated alginate microbeads was controlled by manipulating the beam diameter of the pulsed laser, i.e., the smaller the beam, the smaller the microbead. This was possible down to a threshold laser fluence of approximately 0.11 J/cm^2, below which no

material was deposited. The beam profile was approximately Gaussian, and aided by the intracavity aperture. The beam diameter was controlled using an iris in the beam path close to the objective. After crosslinking the alginate to form microbeads, images were acquired using a Zeiss Z1 microscope with Axiovision software (Carl Zeiss, Thornwood, NY). The laser beam diameter was approximated by measuring the diameter of ink ablated from a glass slide by a laser pulse. Diameters of microbeads were measured using Axiovision.

Each alginate microbead was treated as spherical, and the microbead diameter was measured in Axiovision software. Diameters were averaged for each twelve-bead printed pattern, and the standard deviation was obtained. Statistical analysis was performed in JMP Statistical Discovery Software (version 9, SAS, Cary, NC, USA). A 2-tailed Student's t-test was used to determine the p-value for the effect of the diameter of the laser beam on the diameter of the printed microbead. To measure microbead circularity and pattern fidelity, image analysis tools in ImageJ (US National Institutes of Health Bethesda, MD, USA) were utilized. Images were processed using background subtraction if necessary, edge detection or thresholding, conversion to binary, and successive dilation and filling of holes until all microbead areas were full. For beads that were very close together, this method connected some beads, so the paintbrush tool at single-pixel level and erosion were used for separation of joined microbeads only. The "analyze particles" tool in ImageJ was used determine microbead circularity, centroid locations, and average diameter. Diameter was calculated by averaging the maximum and minimum Feret diameters measured by ImageJ. The distances between microbead centroids were calculated and compared to the desired distance. Microbead circularities and distances within each pattern were averaged.

To visualize the overall 3D structure of the alginate beads, stock fluorescent rhodamine dye in DMSO at 2.5 mg/ml was diluted to a final concentration of 1 μg/ml in 2% alginate/0.9% sodium chloride solution. The alginate droplets were transferred to the receiving substrate as previously described, and incubated for 10 minutes to allow calcium chloride crosslinking of the alginate. Fluorescent microbeads were then visualized using the Zeiss ApoTome and Z-stack imaging in Axiovision software. Fluorescent M231 cells were also visualized in 3D using the ApoTome.

2.4. Analysis of cell viability in microbeads

Live-dead solution was prepared from a Live-Dead Staining Kit (Biovision, Inc., Milpitas, CA), and staining was performed on printed beads at one day, three days, or five days after printing. Culture media was removed from the beads, and beads were incubated for 15 minutes in staining buffer with final concentrations of Live-Dye™ dye at 1 μM to stain live cells, and propidium iodide at 2.5 μg/ml to stain dead cells. The live-dead stain was also performed on cells on the print ribbon immediately after printing. Living cells emitted at 518 nm (green), while dead cells emitted at 615 nm (red).

Live-dead image analysis was performed in ImageJ. The number of cells fluorescing at 518 nm and at 615 nm were counted individually. The percentage of live cells was calculated by the number cells emitting at 518 nm divided by the total number of cells stained.

2.5. Hybrid cell-microbead patterning using LDW

To further demonstrate the utility of this process, hybrid patterns of printed cells and microbeads were created using LDW. Our lab has previously demonstrated the ability to directly pattern cells using gelatin-based LDW, such that cells are printed onto a substrate with unrestricted cell growth following transfer [32]. We modified this method to accommodate the printing of microbeads and cells to the same common substrate. A receiving substrate was prepared by spin coating 10% gelatin/1% calcium chloride to a PLL-

coated Petri dish at 4000 rpm. After five minutes in refrigeration, the Petri dish was washed with 1% calcium chloride/DMEM, and the dish was incubated at 37 °C. To fabricate and localize the microbeads, an initial ribbon was prepared, loaded with M231 cells suspended in 2% alginate, and microbeads were created and deposited using the laser as described above. Prior to bead deposition, a second ribbon was prepared for cellular LDW [32], by spin-coating with 20% gelatin/DMEM and loading with fibroblasts suspended in media. After bead deposition, cells from the second ribbon were patterned into programmed spots within the microbead array. After allowing 15 minutes for cell attachment, media was added to the hybrid pattern to facilitate survival of cells, both the M231 cells within beads and the fibroblasts attached to the substrate. The pattern was imaged immediately after printing and following 24 hours in culture.

3. Results

3.1. Alginate microbead fabrication and characterization

Alginate microbeads were successfully fabricated and patterned in a single step using our laser-based fabrication and deposition method. To demonstrate the repeatability of this technique, we examined the influence of laser beam size on the diameter of laser-fabricated alginate microbeads. A beam diameter of 100 µm produced alginate beads with diameters of 102 ± 8 µm (Fig. 2a). A larger beam (diameter = 175 µm) produced alginate beads with an average diameter of 349 ± 21 µm (Fig. 2b). However, bead fabrication is not limited to these sizes. Rather, beads can be generated outside of this size range by manipulating the size of the laser beam (Fig. 2c). To illustrate the precision and customizability of the technique, representative arrays with 600-µm centroid-to-centroid spacing for both 100-µm-diameter and 350-µm-diameter beads were produced (Fig.2 d–e). The effect of beam width on microbead diameter was statistically significant ($p<0.001$, n=3; Fig. 3).

Although the appearance of cells in multiple planes within microbeads suggested a 3D structure, we confirmed 3D structure using microscopy. Fluorescent rhodamine dye was added to the alginate, and the 3D structure was visualized by acquiring a Z-stack image using the Zeiss ApoTome. An orthogonal view of a microbead suggests a spheroidal 3D structure (Fig. 4a). GFP-expressing M231 cells imaged in 3D were also encapsulated in different planes of the 3D microbead (Fig. 4b).

To demonstrate the precision and micron-level resolution of this printing technique, we patterned beads so that edges were adjacent. Adjacent beads were successfully printed with 100-µm diameter and with 100-µm centroid-to-centroid spacing (Fig. 5a). The printing resolution to deposit adjacent beads for a desired bead size was further demonstrated by printing adjacent beads with 150-µm diameter and 175-µm centroid-to-centroid spacing (Fig. 5b). In all patterns, for all spacings and bead sizes, the average circularity of microbeads was greater than 0.85, and approached 0.9 when microbeads were not adjacent. The precision of centroid-to-centroid microbead spacing was within 2% of the desired spacing, regardless of bead size or pattern spacing (Table 1). To illustrate the scalability of this technique, large patterns in 10×10 arrays were produced. Beads were fabricated and placed at a rate of 1 Hz, a conservative demonstration of the high-throughput capability of the system. The center-to-center bead spacing of these arrays was 600 µm, making each array 5.4 mm × 5.4 mm in size (Fig. 6).

3.2. Cell Viability in Alginate Beads

To ensure that laser-based bead fabrication was not detrimental to encapsulated cells, we measured cell viability before and after bead fabrication using a live-dead staining kit. Cells encapsulated inside of beads were distinguished by cell-permeable fluorescent dye, green for

living, and red for dead. 98% of cells were alive on the print ribbon compared to 89.6% of cells encapsulated in beads one day after printing. Longer-term cell viability was maintained in culture, with a slight decrease over time to 86.7% at 3 days and 84.3% at 5 days (Fig. 7). Encapsulated cells appeared to remain localized within the 2% alginate microbeads, showing no evidence of proliferation or migration over a 7-day period (Fig. 8). However, cells in the alginate microbeads grew up to 40% in diameter over 7 days.

3.3 Compatibility with cellular laser direct-write

We have shown that this technique also enables the hybrid patterning of cells and microbeads together on a common substrate to create hybrid cell-microbead arrays. The fibroblasts and cell-loaded microbeads (M231) were successfully patterned onto a single common substrate in an alternating checkerboard pattern of microbeads and cells, demonstrating the ability to fabricate precise hybrid cell-microbead arrays (Fig. 9). After one day in culture, cells printed by LDW had attached and began to migrate, while cells in microbeads remained encapsulated and immobilized. Moreover, the patterned microbeads maintained their printed locations through the duration in culture. These findings demonstrate that that hybrid constructs can be fabricated in which cells in the same construct can have either unrestricted growth (via gelatin-based LDW of cells) or complete encapsulation and localization (via LDW-microbeads).

4. Discussion

We have demonstrated a novel, single-step method for alginate/calcium chloride microbead fabrication and precise placement using LDW. Fabricated bead diameter is controllable within 8% by adjusting the diameter and fluence of the laser beam, and beads can be placed within 2% of the desired location via CAD/CAM. Precise, single microbead placement has not previously been achieved, and placement is an important step to create spatially-precise constructs to probe basic biology questions involving paracrine signaling or cell-to-cell interactions. The versatility of this technique allows tuning the mechanical properties of the bead by adjusting the alginate and/or calcium chloride concentration. Many current microbead fabrication techniques are limited in their ability to fabricate small beads, and cannot reliably fabricate beads in the 100–300 μm range. Herein, we show that LDW-based bead fabrication can produce and deposit beads over a large range of sizes based on the laser beam energy and iris size. Size control of microbeads will enable the engineering of more precise tissue constructs, and will also allow defined amounts of small molecules to be sequestered and delivered based on their concentration in the alginate and the tunable material properties of the alginate.

Our method represents a fundamental shift from traditional direct-write technologies and printing, where a material is deposited from one planar surface to another. With other direct-write methods, including previous direct-write of microbeads [29], the transfer event deposits material from ribbon to the substrate while preserving the transferred material geometry. With direct-write of a viscous material, the absorption of laser energy causes desorption of the material, which may form a jet or plume as it is deposited [35], though the material will revert to its original planar geometry after it is transferred to the substrate. By contrast, *in situ* crosslinking in our technique alters the geometry of the material from planar while on the ribbon, to 3D after transfer to the substrate, because the geometry of the ejected spheroid droplet is retained during the *in situ* crosslinking event (Fig. 10). Attaining the 3D geometry in a single step results in minimized processing of microbeads and concomitant high cell viability, along with superior localization of microbeads.

Further applications of microbead fabrication and patterning extend to biological studies. In our technique, the high-velocity ejection of alginate into the gelatin substrate, along with *in*

situ crosslinking, allows immobilization of beads in the substrate coating, thus maintaining pattern registry. In contrast, conventional bead fabrication techniques deposit alginate into aqueous calcium chloride solution, and beads are allowed to disperse without any control on placement. In addition to tissue engineering applications, precise placement of beads in patterns lends itself to creating spatially-precise bead arrays/cultures to study cellular signaling. Alginate is commonly used to sequester small molecules and drugs [36], and precise placement of beads with respect to cells offers the potential to study cellular response to a precise, chemotactic signal. By controlling both the concentration of a factor in the bead and the distance from a cell population – either sequestered in a separate bead or adherent to the substrate – the chemical and directional response of cells can be studied.

Microbeads are not limited to sequestering small molecules. They can also encapsulate cells that continue to produce factors at a steady state, unlike the exponential decay release profile typical of sequestered molecules. In this study, we observed viable encapsulated cells out to 5 days, and other studies have shown continued release of growth factors after weeks in alginate-encapsulated cells [14]. Cell viability within beads of 89.6% is comparable to cell printing using LDW [32,33], as well as viability demonstrated by other techniques [8], although many studies do not report a value for viability. This high cell viability is also achieved in single-step fabrication and patterning, while the viability is much lower when fabrication and patterning is performed in two steps [29]. This high viability enables this laser-based bead fabrication technique to be used for tissue engineering purposes. Additionally, the cells encapsulated in microbeads were able to grow in size throughout their time in culture, yet remained immobilized within the non-functionalized alginate matrix, showing no evidence of migration or proliferation (Fig. 8). This could possibly be due to the dense 2% alginate hydrogel [37], or the lack of sites for cell attachment. If cell proliferation within the beads is desired, a modified alginate can be used (e.g., RGD-functionalized alginate) that provides sites for cell attachment. Microbeads can also be further processed to allow cell attachment or to dissociate the alginate on the inside of beads, enabling cell attachment to the hollow shell [38]. Some bead materials, such as alginate-fibrin, allow encapsulation and quick release of cells compared to alginate alone [39].

The high-throughput capabilities and versatility of LDW make it a valuable tool for rapidly fabricating microbeads. In this study, microbeads were precisely fabricated and patterned at 1 Hz, though the laser has a 300 Hz repetition rate. Deposition speed can be increased by both increasing the laser repetition rate and increasing the stage velocity and/or decreasing the distance between printed beads. For scaling production of microbeads, alginate can be deposited into a calcium chloride bath, where alginate beads can rapidly be generated and recovered. Recovered beads can then be stored in cell culture media in an incubator for use at a later desired time.

Consistent microbead placement, within 2% of desired location, was demonstrated by patterning beads in rectangular grids, and edge-to-edge placement of 100-μm diameter beads (Fig. 5a) illustrates the repeatability of the technique. There was little loss of microbead fidelity with edge-to-edge placement, as average circularity remained above 0.85 (Table 1). However, some changes in microbead appearance and deformation were observed with edge-to-edge placement, and we suspect these resulted from physical interactions with adjacent beads. Nevertheless, precise edge-to-edge placement also suggests that bead placement can be adapted to custom-printed constructs where the microbeads serve as volume pixels, or "voxels." Extrapolation of this technique could be used for the fabrication of 3-D structures where each bead location could be tailored to hold a specific cell type or soluble factor in the structure. The use of multiple cell types would enable complex, customizable, bottom-up tissue engineering. Moreover, the high surface area-to-volume

ratio of the beads may allow for nutrient exchange through the 3D structure with better efficiency than bulk hydrogel scaffolds provide.

We have additionally shown that traditional gelatin-based laser direct-write for cell patterning [32] is compatible with the alginate bead fabrication. The ability to deposit cells along with beads in a predetermined array offers exciting experimental potential for researching cell migration in correspondence to spatial cues, soluble factor gradients, and drug delivery. With the combination of these tools, we have the capability to selectively put cells in either 2D or 3D environments, thereby affecting the cellular microenvironment and influencing cell behaviour [40,41].

Further processing of alginate microbeads with poly-L-lysine (PLL) or chitosan can be used to form a shell around the microbeads, altering their material properties [42–44]. With the addition of sodium citrate, the alginate can be liquefied with the shell intact, forming a microcapsule. Interaction with the shell in an aqueous environment allows cellular migration and proliferation that alginate encapsulation inhibits, while still maintaining a physical constraint on migration so that cells can be localized to a desired area. Localization of microcapsules has not been previously demonstrated. Alginate has shown great utility for both microbead and microcapsule formation [42,45].

Furthermore, unlike electrostatic bead generation techniques, which rely on the charge of the polymer for mass transfer, LDW is not limited by the charge of the material. In theory, microbead fabrication based on LDW can be applied to transfer any UV-absorptive material onto a substrate with its corresponding cross-linker. This versatility may enable the use of a wide range of biomaterials including chitosan [46], thrombin [39,47], and hyaluronan [9,48]. UV-photocrosslinkable materials [39,49] could potentially be used as well, because this technique utilizes a UV laser. A wide range of potential materials, coupled with the combination of size and placement control of microbeads, makes this technique very powerful for tissue engineering applications.

5. Conclusions

Laser direct-write is a powerful tool for precise alginate microbead fabrication, reproducibly making beads from 100 to 500 μm, and potentially outside this range by adjusting the laser beam diameter. Microbeads were fabricated and placed in a single-step process, using the standard LDW setup, to rapidly generate spatially-precise arrays. This technique has demonstrated the ability to load beads with soluble factors or encapsulate cells. Further, the cells encapsulated in the fabricated microbeads maintained a high viability after the process was completed. Laser-based microbead deposition is compatible with LDW for cell deposition, making it now possible to create customizable arrays of cells and microbeads. Applications of this method include studies involving cell-cell interactions, controlled drug delivery over a specified distance, soluble factor gradients to direct migration, bottom-up tissue engineering, and countless other studies or approaches.

Acknowledgments

References

1. Xie Y, Castracane J. High-voltage, electric field-driven micro/nanofabrication for polymeric drug delivery systems. Engineering in Medicine and Biology. 2009; 28:23–30.

2. Gombotz WR, Wee SF. Protein release from alginate matrices. Advanced Drug Delivery Reviews. 2012; 64:194–205.

3. Mørch YA, Donati I, Strand BL, Skjåk-Braek G. Effect of Ca2+, Ba2+, and Sr2+ on alginate microbeads. Biomacromolecules. 2006; 7:1471–1480. [PubMed: 16677028]

4. Rokstad AM, Brekke OL, Steinkjer B, Ryan L, Kolláriková G, Strand BL, Skjåk-Bræk G, Lacík I, Espevik T, Mollnes TE. Alginate microbeads are complement compatible, in contrast to polycation containing microcapsules, as revealed in a human whole blood model. Acta Biomaterialia. 2011; 7:2566–2578. [PubMed: 21402181]

5. Robert D, Fayol D, Le Visage C, Frasca G, Brulé S, Ménager C, Gazeau F, Letourneur D, Wilhelm C. Magnetic micro-manipulations to probe the local physical properties of porous scaffolds and to confine stem cells. Biomaterials. 2010; 31:1586–1595. [PubMed: 19932922]

6. Kong HJ, Kaigler D, Kim K, Mooney DJ. Controlling rigidity and degradation of alginate hydrogels via molecular weight distribution. Biomacromolecules. 2004; 5:1720–1727. [PubMed: 15360280]

7. De Groot M, Keizer PP, de Haan BJ, Schuurs TA, Leuvenink HG, van Schilfgaarde R, de Vos P. Microcapsules and their ability to protect islets against cytokine-mediated dysfunction. Transplantation Proceedings. 2001; 33:1711–1712. [PubMed: 11267481]

8. Huang X, Zhang X, Wang X, Wang C, Tang B. Microenvironment of alginate-based microcapsules for cell culture and tissue engineering. Journal of Bioscience and Bioengineering. 2012; 114:1–8. [PubMed: 22561878]

9. Drury JL, Mooney DJ. Hydrogels for tissue engineering: scaffold design variables and applications. Biomaterials. 2003; 24:4337–4351. [PubMed: 12922147]

10. Loh QL, Wong YY, Choong C. Combinatorial effect of different alginate compositions, polycations, and gelling ions on microcapsule properties. Colloid and Polymer Science. 2012; 290:619–629.

11. Vandenberg GW, Drolet C, Scott SL, de la Noüe J. Factors affecting protein release from alginate-chitosan coacervate microcapsules during production and gastric/intestinal simulation. Journal of Controlled Release. 2001; 77:297–307. [PubMed: 11733097]

12. Tan WH, Takeuchi S. Monodisperse Alginate Hydrogel Microbeads for Cell Encapsulation. Advanced Materials. 2007; 19:2696–2701.

13. Wu MH, Pan WC. Development of microfluidic alginate microbead generator tunable by pulsed airflow injection for the microencapsulation of cells. Microfluidics and Nanofluidics. 2009; 8:823–835.

14. Hunt NC, Shelton RM, Henderson DJ, Grover LM. Calcium-alginate hydrogel-encapsulated fibroblasts provide sustained release of vascular endothelial growth factor. Tissue Engineering: Part A. 2012; 19:905–914. [PubMed: 23082964]

15. Magyar JP, Nemir M, Ehler E, Suter N, Perriard JC, Eppenberger HM. Mass production of embryoid bodies in microbeads. Annals of the New York Academy of Sciences. 2001; 944:135–143. [PubMed: 11797664]

16. Zhang X, Xie Y, Koh CG, James Lee L. A novel 3-D model for cell culture and tissue engineering. Biomedical Microdevices. 2009; 11:795–799. [PubMed: 19288199]

17. Sayyar B, Dodd M, Wen J, Ma S, Marquez-Curtis L, Janowska-Wieczorek A, Hortelano G. Encapsulation of factor IX-engineered mesenchymal stem cells in fibrinogen-alginate microcapsules enhances their viability and transgene secretion. Journal of Tissue Engineering. 2012

18. Wang Y, Irvine D. Engineering chemoattractant gradients using chemokine-releasing polysaccharide microspheres. Biomaterials. 2012; 32:4903–4913. [PubMed: 21463892]

19. Zhao X, Jain S, Benjamin Larman H, Gonzalez S, Irvine DJ. Directed cell migration via chemoattractants released from degradable microspheres. Biomaterials. 2005; 26:5048–5063. [PubMed: 15769541]

20. Ciofani G, Raffa V, Menciassi A, Micera S, Dario P. A drug delivery system based on alginate microspheres: mass-transport test and in vitro validation. Biomedical Microdevices. 2007; 9:395–403. [PubMed: 17252208]

21. Tsuda Y, Morimoto Y, Takeuchi S. Monodisperse cell-encapsulating peptide microgel beads for 3D cell culture. Langmuir. 2010; 26:2645–2649. [PubMed: 19845343]

22. Choi CH, Jung JH, Rhee YW, Kim DP, Shim SE, Lee CS. Generation of monodisperse alginate microbeads and in situ encapsulation of cell in microfluidic device. Biomedical microdevices. 2007; 9:855–862. [PubMed: 17578667]

23. Huang, S Bin; Wu, MH.; Lee, G Bin. Microfluidic device utilizing pneumatic microvibrators to generate alginate microbeads for microencapsulation of cells. Sensors and Actuators B: Chemical. 2010; 147:755–764.

24. Desmarais SM, Haagsman HP, Barron AE. Microfabricated devices for biomolecule encapsulation. Electrophoresis. 2012; 33:2639–2649. [PubMed: 22965707]

25. Moya ML, Morley M, Khanna O, Opara EC, Brey EM. Stability of alginate microbead properties in vitro. Journal of Material Science: Material Medicine. 2012; 23:903–912.

26. Sohail A, Turner MS, Coombes A, Bostrom T, Bhandari B. Survivability of probiotics encapsulated in alginate gel microbeads using a novel impinging aerosols method. International Journal of Food Microbiology. 2011; 145:162–168. [PubMed: 21276627]

27. Zhang Q, Xu J-J, Chen H-Y. Patterning microbeads inside poly(dimethylsiloxane) microfluidic channels and its application for immobilized microfluidic enzyme reactors. Electrophoresis. 2006; 27:4943–4951. [PubMed: 17117456]

28. Lin YH, Yang YW, Chen YD, Wang SS, Chang YH, Wu MH. The application of an optically switched dielectrophoretic (ODEP) force for the manipulation and assembly of cell-encapsulating alginate microbeads in a microfluidic perfusion cell culture system for bottom-up tissue engineering. Lab Chip. 2012; 12:1164–1173. [PubMed: 22322420]

29. Phamduy TB, Raof NA, Schiele NR, Yan Z, Corr DT, Huang Y, Xie Y, Chrisey DB. Laser direct-write of single microbeads into spatially-ordered patterns. Biofabrication. 2012; 4:025006. [PubMed: 22556116]

30. Palla-Papavlu A, Dinca V, Paraico I, Moldovan A, Shaw-Stewart J, Schneider CW, Kovacs E, Lippert T, Dinescu M. Microfabrication of polystyrene microbead arrays by laser induced forward transfer. Journal of Applied Physics. 2010; 108:033111.

31. Lin Y, Huang Y. Laser-assisted fabrication of highly viscous alginate microsphere. Journal of Applied Physics. 2011; 109:083107.

32. Schiele NR, Chrisey DB, Corr DT. Gelatin-based laser direct-write technique for the precise spatial patterning of cells. Tissue Engineering Part C: Methods. 2011; 17:289–298. [PubMed: 20849381]

33. Raof NA, Schiele NR, Xie Y, Chrisey DB, Corr DT. The maintenance of pluripotency following laser direct-write of mouse embryonic stem cells. Biomaterials. 2011; 32:1802–1808. [PubMed: 21168910]

34. Gruene M, Deiwick A, Koch L, Schlie S, Unger C, Hofmann N, Bernemann I, Glasmacher B, Chichkov B. Laser printing of stem cells for biofabrication of scaffold-free autologous grafts. Tissue Engineering Part C: Methods. 2011; 17:1–36.

35. Young D, Auyeung RCY, Piqué A, Chrisey DB, Dlott DD. Plume and jetting regimes in a laser based forward transfer process as observed by time-resolved optical microscopy. Applied Surface Science. 2002; 198:181–187.

36. Amsden BG, Goosen MFA. An examination of factors affecting the size, distribution and release characteristics of polymer microbeads made using electrostatics. Journal of Controlled Release. 1997; 43:183–196.

37. Zhang J, Yang Z, Li C, Dou Y, Li Y, Thote T, Wang D, Ge Z. Cells Behave Distinctly Within Sponges and Hydrogels Due to Differences of Internal Structure. Tissue Engineering: Part A. 2013; 19:2166–2175. [PubMed: 23614637]

38. Yu J, Du KT, Fang Q, Gu Y, Mihardja SS, Sievers RE, Wu JC, Lee RJ. The use of human mesenchymal stem cells encapsulated in RGD modified alginate microspheres in the repair of myocardial infarction in the rat. Biomaterials. 2010; 31:7012–7020. [PubMed: 20566215]

39. Zhou H, Xu HHK. The fast release of stem cells from alginate-fibrin microbeads in injectable scaffolds for bone tissue engineering. Biomaterials. 2011; 32:7503–7513. [PubMed: 21757229]

40. Cukierman E, Pankov R, Stevens DR, Yamada KM. Taking cell-matrix adhesions to the third dimension. Science. 2001; 294:1708–1712. [PubMed: 11721053]

41. Khademhosseini A, Langer R, Borenstein J, Vacanti JP. Microscale technologies for tissue engineering and biology. PNAS. 2006; 103:2480–2487. [PubMed: 16477028]

42. Orive G, Tam SK, Pedraz JL, Hallé JP. Biocompatibility of alginate-poly-L-lysine microcapsules for cell therapy. Biomaterials. 2006; 27:3691–3700. [PubMed: 16574222]

43. King GA, Daugulis AJ, Faulkner P, Goosen MFA. Alginate-polylysine microcapsules of controlled membrane molecular weight cutoff for mammalian cell culture engineering. Biotechnology Progress. 1987; 3:231–240.

44. Chen H, Ouyang W, Lawuyi B, Prakash S. Genipin cross-linked alginate-chitosan microcapsules: membrane characterization and optimization of cross-linking reaction. Biomacromolecules. 2006; 7:2091–2098. [PubMed: 16827575]

45. Wang W, Liu X, Xie Y, Zhang H, Yu W, Xiong Y, Xie W, Ma X. Microencapsulation using natural polysaccharides for drug delivery and cell implantation. Journal of Materials Chemistry. 2006; 16:3252.

46. Mark D, Haeberle S, Zengerle R, Ducree J, Vladisavljevi GT. Manufacture of chitosan microbeads using centrifugally driven flow of gel-forming solutions through a polymeric micronozzle. Journal of Colloid and Interface Science. 2009; 336:634–641. [PubMed: 19428020]

47. Gruene M, Pflaum M, Hess C, Diamantouros S, Schlie S, Deiwick A, Koch L, Wilhelmi M, Jockenhoevel S, Haverich A, Chichkov B. Laser printing of three-dimensional multicellular arrays for studies of cell-cell and cell-environment interactions. Tissue Engineering Part C: Methods. 2011; 17:973–982. [PubMed: 21585313]

48. Tan H, Chu CR, Payne KA, Marra KG. Injectable in situ forming biodegradable chitosan-hyaluronic acid based hydrogels for cartilage tissue engineering. Biomaterials. 2009; 30:2499–2506. [PubMed: 19167750]

49. Liu WF, Chen CS. Cellular and multicellular form and function. Advanced Drug Delivery Reviews. 2007; 59:1319–1328. [PubMed: 17884241]
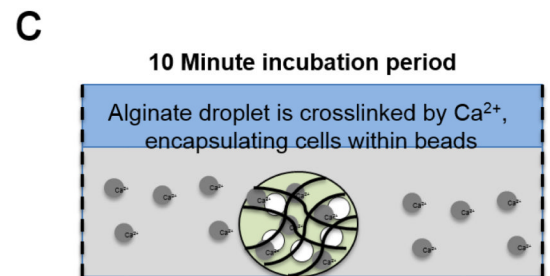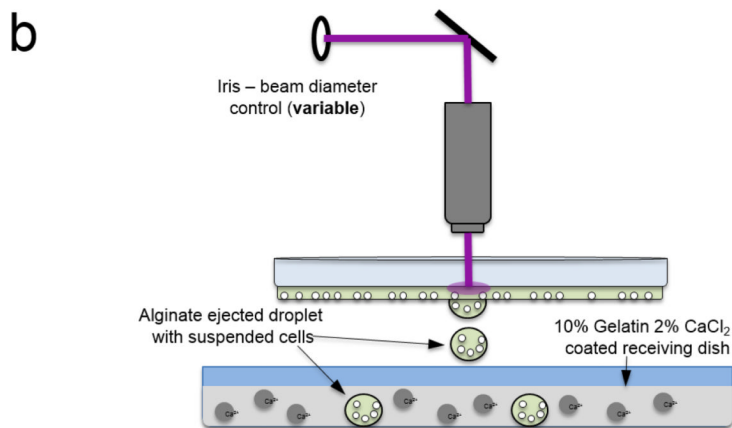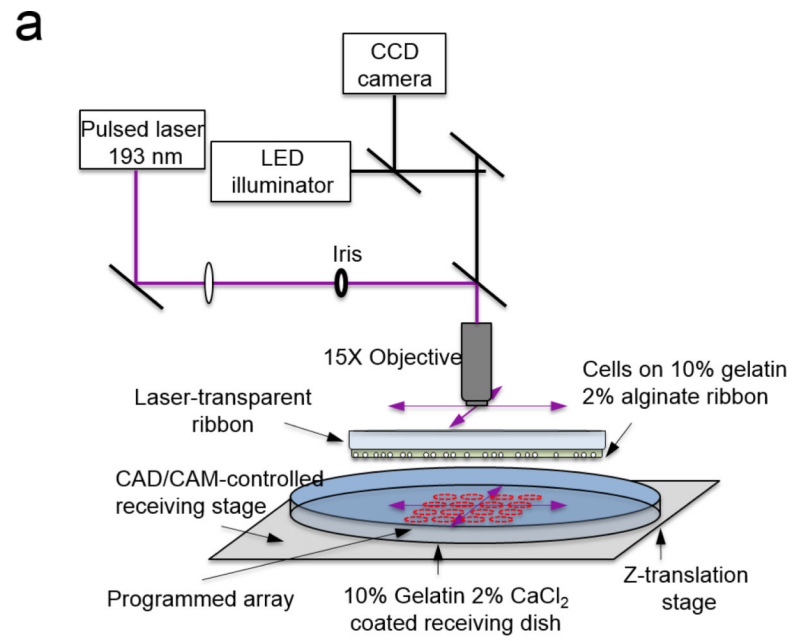
Figure 1.
Schematic of single-step laser-based bead fabrication and deposition process. (a) System overview, (b) alginate droplet ejection, and (c) *in situ* crosslinking of microbead.
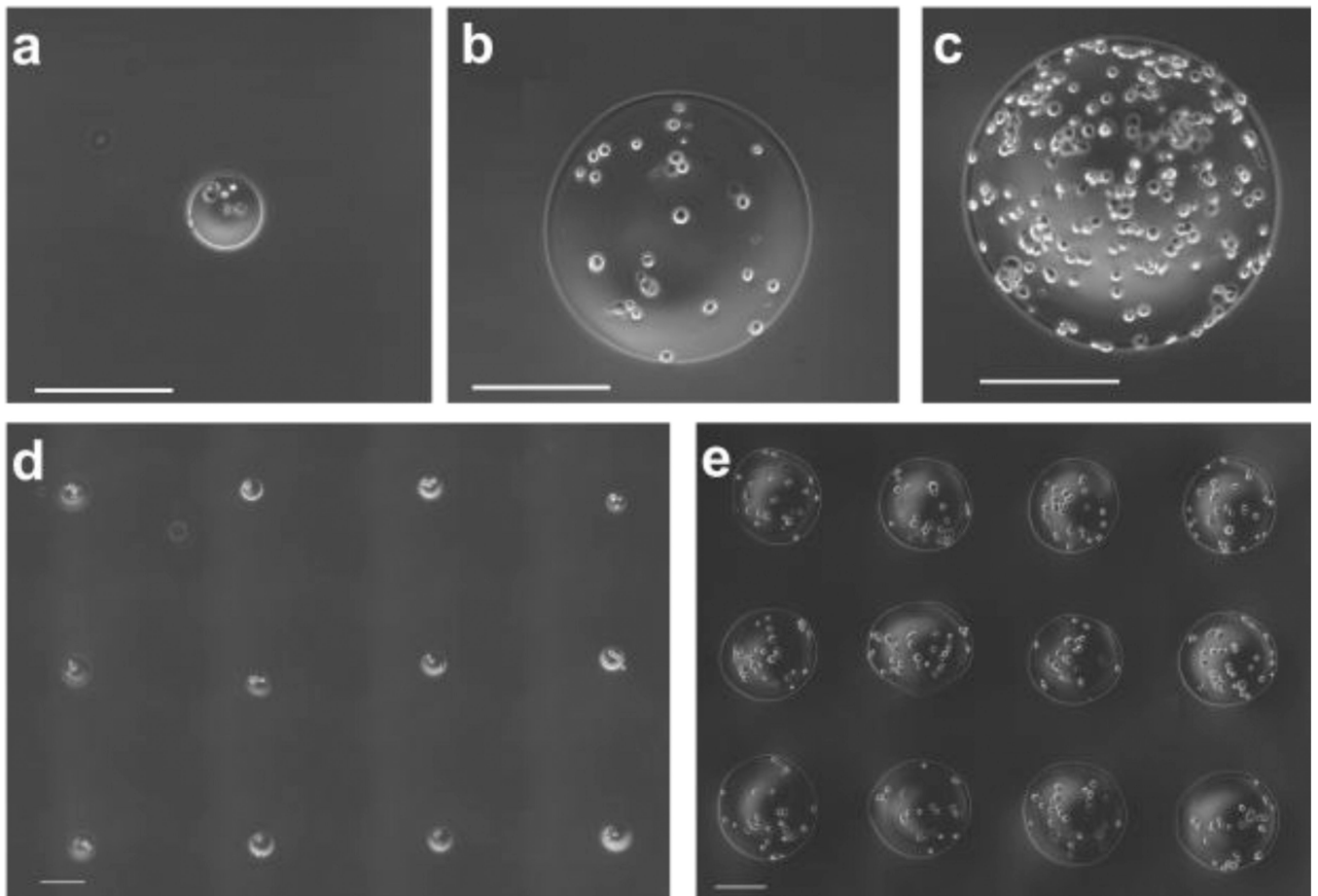
Figure 2.
Laser-fabricated microbeads; (a) Single 100-μm diameter microbead with encapsulated
M231 cells. (b) Single 350-μm-diameter microbead with encapsulated M231 cells. (c) Single
500-μm-diameter microbead with encapsulated M231 cells. Representative pattern of (d)
100-μm-diameter microbeads with encapsulated cells and (e) 350-μm-diameter microbeads
with encapsulated cells. Scale bars are 200 μm.
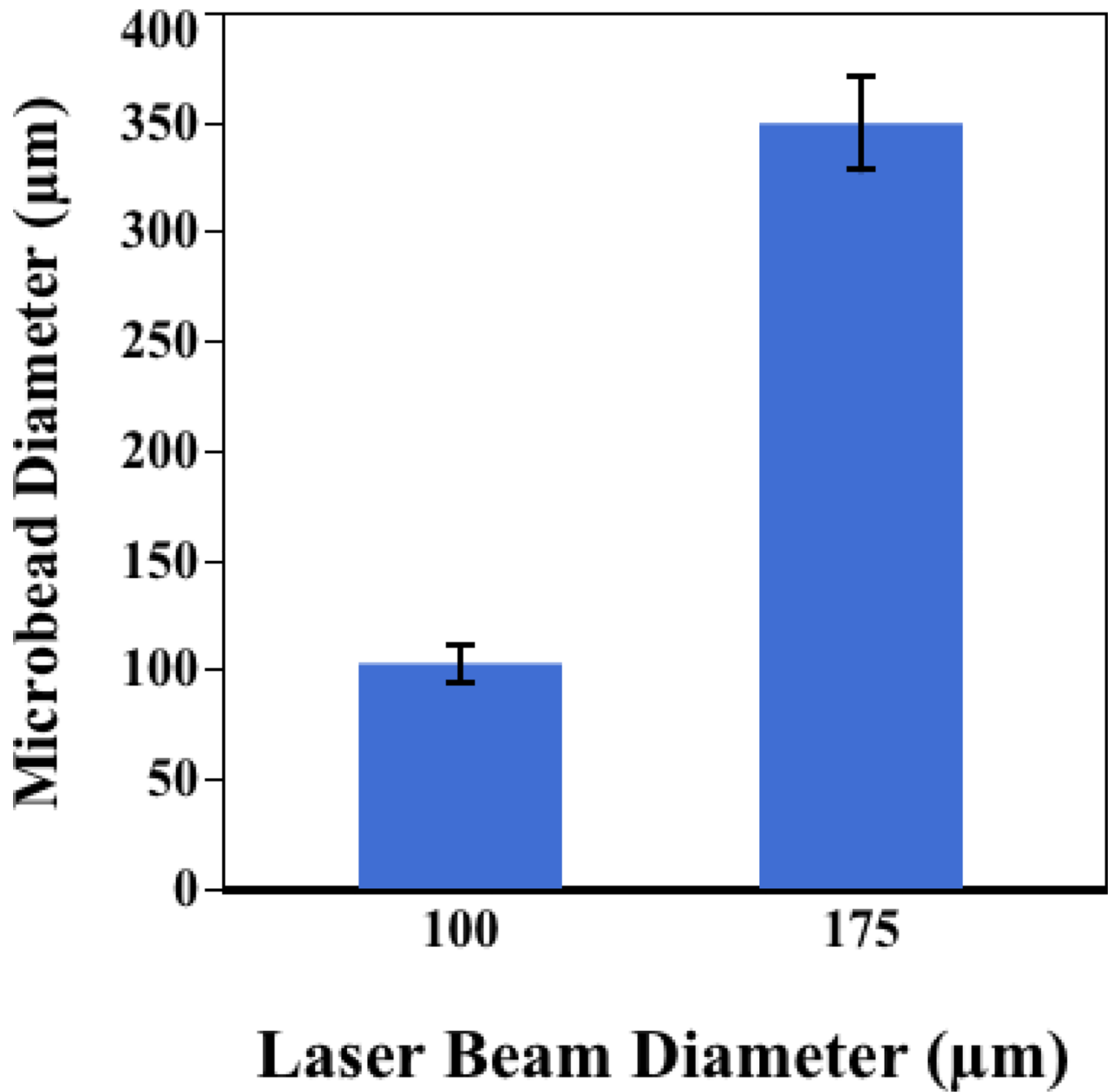
Figure 3.
Influence of laser beam size on fabricated bead diameter. Error bars are one standard deviation.
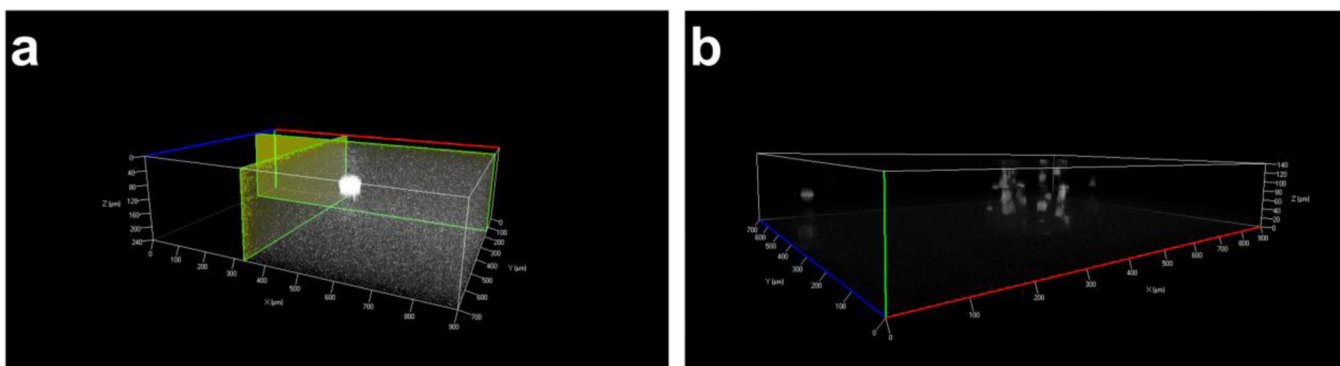
Figure 4.
3-D ApoTome z-stack images of laser-fabricated microbeads (a) with rhodamine dye dissolved in alginate and (b) with GFP-fluorescent M231 cells.
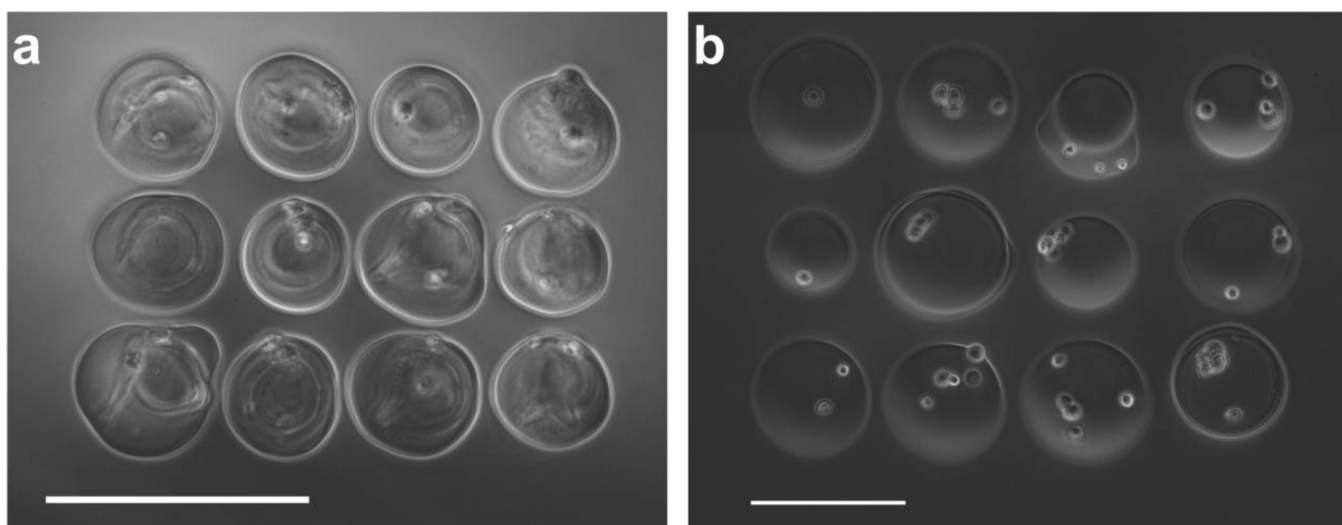
Figure 5.
Grid patterns of adjacent microbeads with (a) 100-μm-diameter microbeads in a grid with 100-μm spacing between microbead centroids and (b) 150-μm-diameter microbeads in a grid with 175-μm spacing between microbead centroids. Scale bars are 200 μm.
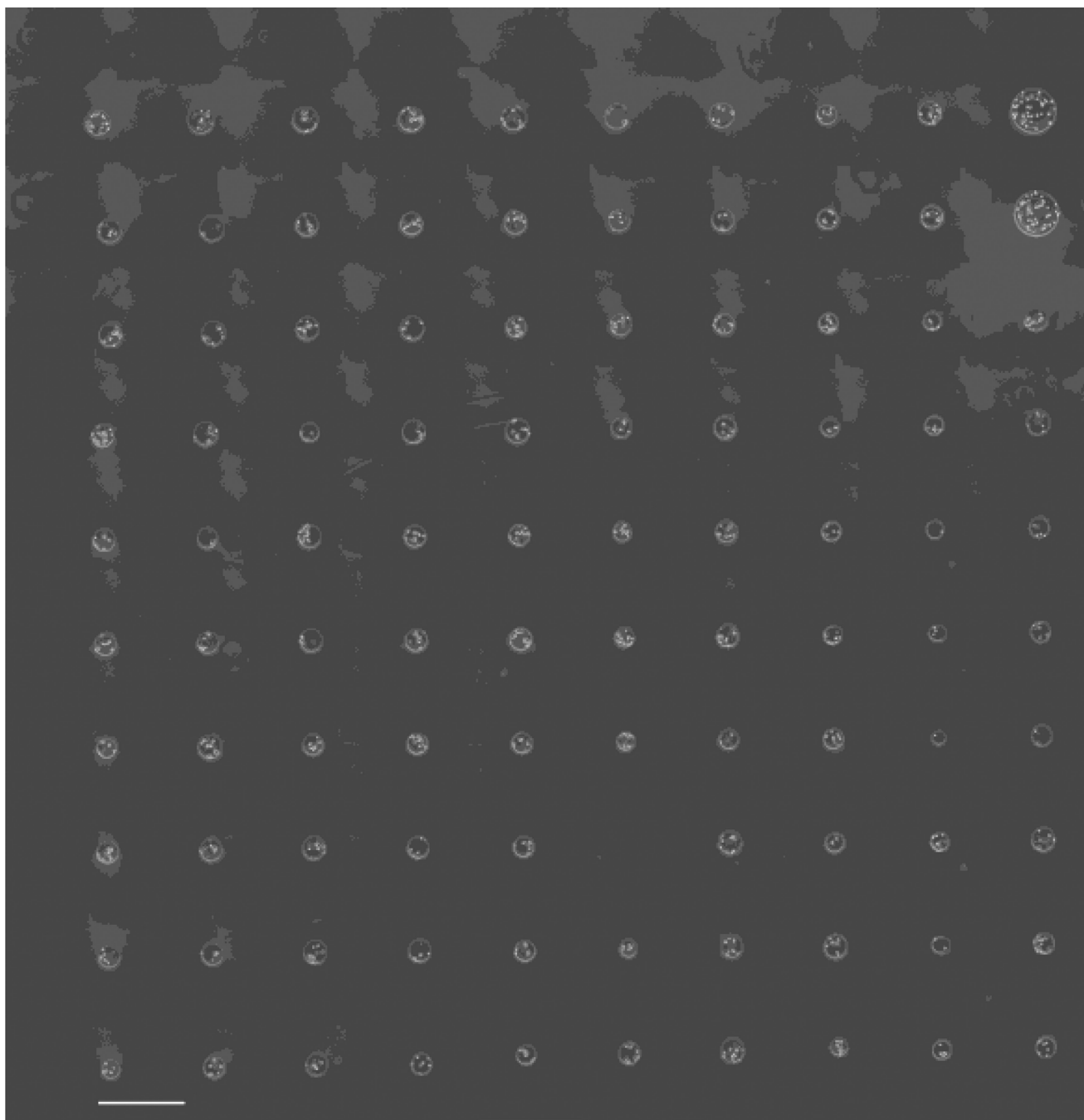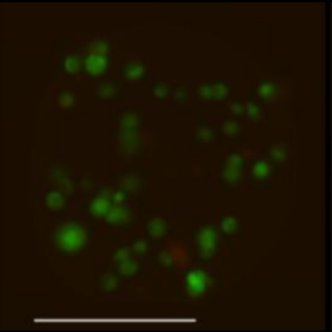
Figure 6.
10×10 array of microbeads. Scale bar is 500 μm.
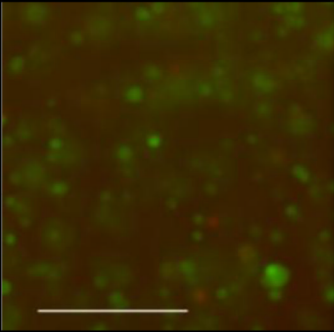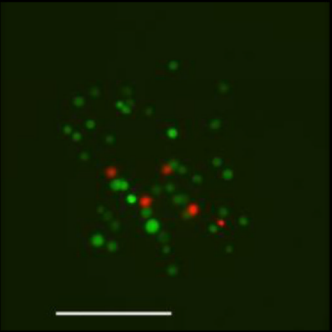
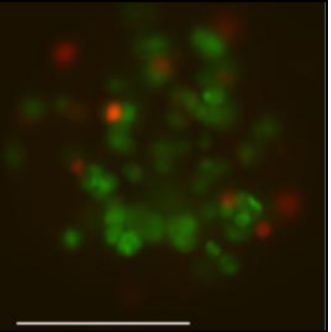| Ribbon	Day 1	Day 3	Day 5
98%	89.7%	86.7%	84.3%

Figure 7.
Live-dead stain of M231 cells showing viability on the print ribbon (day 0), and in representative printed microbeads after 1, 3, and 5 days in culture (green live, red dead). Scale bars are 200 μm.
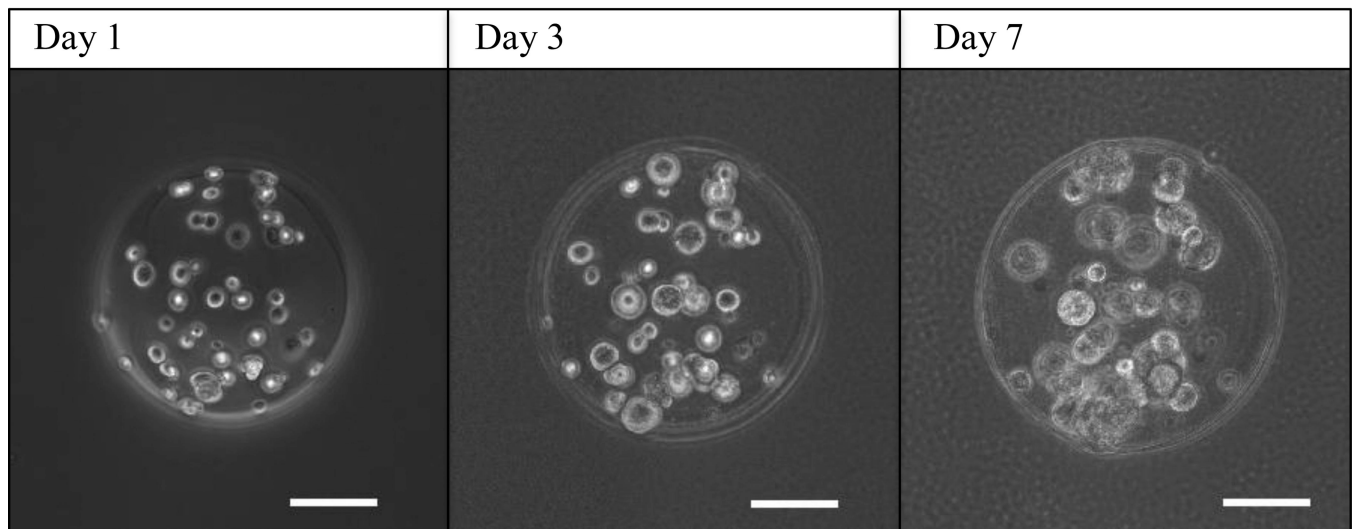
Day 1	Day 3	Day 7

Figure 8.
Time-lapse images of a single microbead over 7 days, illustrating that cells encapsulated inside of microbeads grow in size, while maintaining their relative position. Over time in culture, the cells are able to survive and grow, yet are immobilized within the alginate bead, showing no evidence of either migration or proliferation. Scale bars are 100 μm.
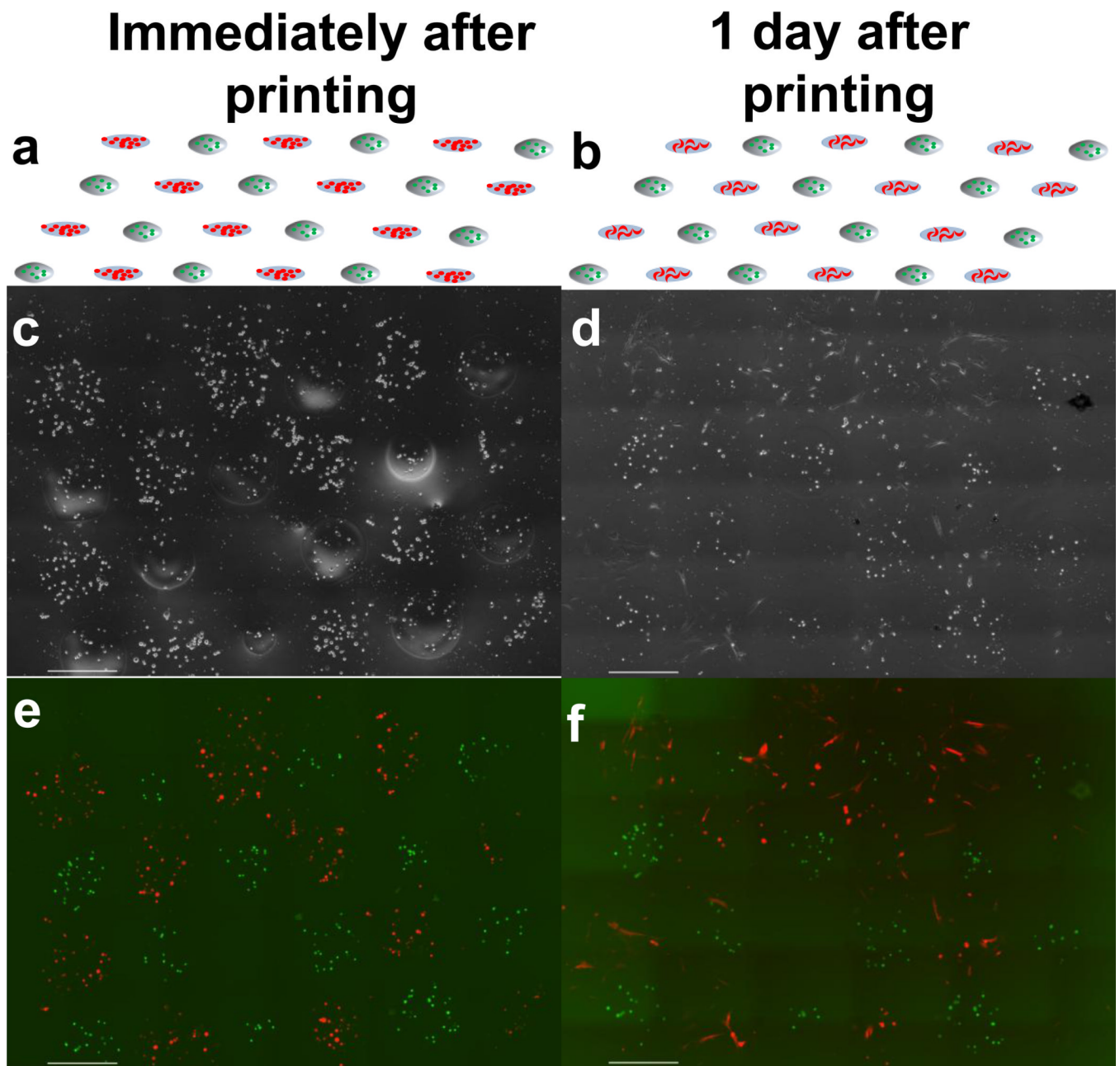
Figure 9.
Schematics and images of hybrid cell/microbead array on glass cover slip shown immediately after printing (a, c, e) and after one day (b, d, f). Schematics (a, b) show the desired alternating checkerboard pattern of M231 cells (green) encapsulated in microbeads and fibroblasts (red) printed directly on the common substrate. Phase contrast images (c, d) and fluorescent images (e, f) show the printed hybrid cell/microbead construct immediately after printing (c, e), and that after 1 day in culture (d, f) the M231 cells remain encapsulated and localized within the microbeads, while growth of fibroblasts is unrestricted. Scale bar is 500 μm.

Laser energy absorption causes vapor pocket and droplet ejection from planar layer on ribbon

Ribbon

Surface tension and cohesion ensure droplet formation

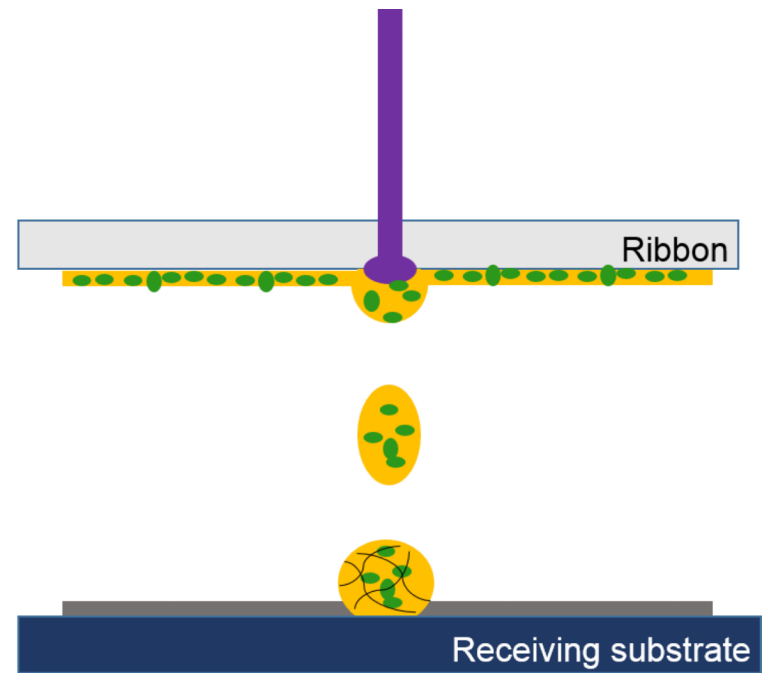*In situ* Ca²⁺ crosslinking of droplet maintains 3D geometry, a fundamental difference from traditional direct-write

Receiving substrate

Figure 10.
Proposed mechanism of laser-based bead fabrication by droplet ejection and *in situ* crosslinking.

Table 1

Characteristics of patterns and microbeads, illustrating fidelity of the technique.

Desired spacing between beads (μm)	Actual average spacing between beads (μm) ± standard deviation	Difference from desired spacing (%)	Average microbead circularity ± standard deviation	Desired microbead diameter	Average microbead diameter (μm) ± standard deviation
100	101.50 ± 2.56	1.53	0.86 ± 0.05	Small	99.74 ± 9.77
300	301.55 ± 4.42	0.52	0.86 ± 0.04	Medium	162.52 15.20
600	601.01 ±13.47	0.17	0.90 ± 0.01	Large	401.57 ± 21.09
600	602.50 ± 4.95	0.42	0.85 ± 0.04	Small	95.85 ± 11.98